IEEE Access
Multidisciplinary | Rapid Review | Open Access Journal

Received May 15, 2018, accepted June 6, 2018, date of publication June 21, 2018, date of current version July 12, 2018.

Digital Object Identifier 10.1109/ACCESS.2018.2848306

Performance Analysis of a Dual-Hop Wireless-Power Line Mixed Cooperative System

AASHISH MATHUR[1], (Member, IEEE), MANAV R. BHATNAGAR[2], (Senior Member, IEEE), YUN AI[3], (Member, IEEE), AND MICHAEL CHEFFENA[3]

[1]Department of Electrical Engineering, IIT Jodhpur, Jodhpur 342037, India
[2]Department of Electrical Engineering, IIT Delhi, New Delhi 110016, India
[3]Faculty of Engineering, Norwegian University of Science and Technology, 2815 Gjøvik, Norway

Corresponding authors: Aashish Mathur (aashishmathur@iitj.ac.in) and Yun Ai (yun.ai@ntnu.no)

ABSTRACT Wireless communications and power line communications (PLC) are essential components for smart grid communications. This paper analyses the performance of a dual-hop wireless-power line mixed communication setup employing a decode-and-forward relay in terms of analytical average bit error rate (BER), outage probability, and average channel capacity. The Nakagami-*m* distribution captures the wireless channel fading; whereas the PLC channel gain is characterized by the Log-normal distribution. The additive PLC channel noise is assumed to be Bernoulli-Gaussian distributed. Approximate closed-form expression of the average BER and exact closed-form expression of the outage probability are derived for the considered system. Further, we obtain an approximate closed-form expression of the capacity of the wireless-power line mixed system in terms of the Meijer-G function. It is observed that the system performance deteriorates as the impulsive noise index and the arrival probability of the impulsive component of the PLC additive noise increase.

INDEX TERMS Bit error rate, Bernoulli-Gaussian noise, channel capacity, decode-and-forward, Nakagami-*m* distribution, Log-normal distribution, outage probability, power line communications.

I. INTRODUCTION

Power line communications (PLC) is being widely used today to meet the ever increasing user demand for speedy access to data [1]. This is primarily because power lines are readily available and cover huge geographical area. However, PLC has its own set of challenges. Since the power lines were not initially designed for communication purposes, there are behavioral differences between a PLC channel and a conventional wired communication channel. As a result, the PLC channel offers a harsh medium for communication signals. Moreover, the channel impedance, noise, and attenuation in PLC systems randomly fluctuate as the time, frequency, and location vary. Therefore, it is a challenging task to model PLC channels [2].

The additive noise in PLC systems is a mixture of background noise and impulsive noise, whose statistical features are described by the Nakagami-*m* distribution [3], [4] and Middleton class A distribution [5], [6], respectively. A maximum likelihood (ML) detector of binary phase shift keying (BPSK) transmitted signals over Nakagami-*m* background noise was evaluated for a PLC system in [7] and its analytical bit error rate (BER) was obtained. In [8], symbol error rate (SER) and BER for a PLC system subjected to Nakagami-*m* noise were derived for quadrature phase shift keying (QPSK) modulation. Recently in [9], the analytical average BER was evaluated for a PLC system under the combined impact of Nakagami-*m* distributed background noise and Middleton class A distributed impulsive noise. Besides the aforementioned noise models, Bernoulli-Gaussian distribution is also a largely followed noise model in PLC literature that includes the effects of both types of additive noises in PLC systems [10], [11].

PLC channel is also effected by multiplicative noise due to the adverse influence of multipath and mismatches in the impedances at the joints. Both Rician and Rayleigh channel models are applicable to PLC systems as justified in [12]–[15]. In [16], PLC system performance corrupted by Rayleigh distributed channel gain over Nakagami-*m* additive background noise was analyzed in terms of BER and outage probability. Besides Rician and Rayleigh channel models, it has also been proposed that the amplitude gain of the PLC channel follows the Log-normal distribution [17]–[19]. The measurement campaign conducted in US urban and sub-urban homes over low and medium voltage power lines

across frequencies of 1.8 MHz to 30 MHz in [18] suggested that the Log-normal distribution indeed models PLC channel gain. In [19], a two-conductor transmission line approach for cabling components was used to model the PLC channel transfer function on account of multipath propagation and the path amplitudes were demonstrated to follow the Log-normal distribution. On the other hand, the Nakagami-*m* fading model is assumed for the wireless channel [20]–[23] as it is possible to describe other fading distributions using the *m* parameter. The noise in a wireless communication system is largely modeled by the additive white Gaussian noise (AWGN).

Motivation: Wireless-power line mixed communication systems have grabbed the attention of the researchers over the years [24]–[26]. It is shown in [25] that the physical layer performance can be improved by using a wireless-power line diversity system by employing diversity combining of the received wireless and PLC signals. In [26], the use of PLC to assist cooperative wireless relaying is investigated, where power lines initialize and synchronize wireless amplify-and-forward relays and broadcast data between these relays. A relay-enabled wireless-PLC system is considered in [27] where a master node communicates with the relay on a wireless link while the relay node communicates with the slave node on a PLC link. Wireless and PLC technologies have also been combined by INSTEON Technology where the wireless technology is mainly used to relay control commands and extend the scale of a control network [28]. In the smart metering approach proposed in [29], the smart meter data collected by the concentration and communication node is sent to the other side of 20/0.4 kV substation using Wi-Fi transceiver. Using a PLC modem, the transmitted data is then launched on high voltage power line and is sent to the 63/20 kV substation. In [30], a software defined networking (SDN) router is used that receives data from sensors wirelessly and transmits the data on a PLC network thereby creating a combined wireless and PLC smart network for a smart home.

The cost of implementation and maintenance of fiber optic link is high. Moreover, Wi-Fi signals can be lost due to the presence of thick brick walls and Wi-Fi dead zones. Therefore, the combined deployment of PLC and wireless system is a potential solution to provide cost-efficient and ubiquitous Internet access in some scenarios. The Internet of Things (IoT) is an upcoming system with a wide range of applications where communication forms a bridge to bond sensors, actuators, control systems, smart devices etc. Both wireless and PLC are essential communication technologies for IoT. However, using stand-alone wireless communication or PLC is quite challenging in an IoT network. Due to the physical connections between the PLC transceivers and the electrical power grid, it is difficult for mobile users to connect to a PLC network [31] whereas, stand-alone wireless communications is not preferable for the smart home networks because many intelligent appliances and sensors, such as energy consumption monitors and multimedia devices,

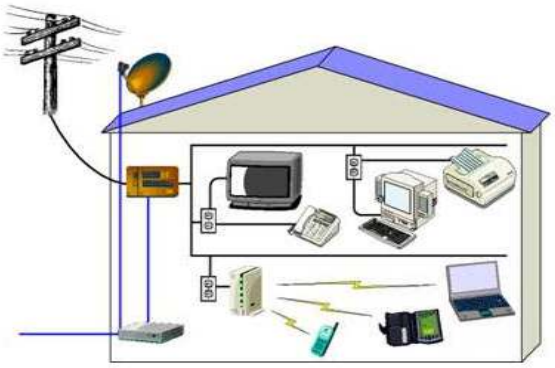

FIGURE 1. Application scenario of a wireless-PLC mixed communication system [34].

require connections to the household alternating current (AC) power distribution network for practical implementation [25]. In this scenario, a mixed wireless and power line communication system is an effective solution for IoT systems [32]. There are many old buildings and homes that are suitable for wireless systems and cannot provide infrastructure capability for smart home environment [30]. In order to integrate such old buildings with the smart grid and to provide last-mile internet access, a mixed wireless-PLC system is required.

According to the International Telecommunication Union (ITU), around 50% of worldwide population are still unconnected and most of them live in the least developed countries in Africa [33]. Building fiber optics and mobile broadband will be extremely expensive for them due to the vast area of Africa (which indicates a lot of investments) and affordability of the advanced technologies. The good news is that most of the people in the least developed countries have already access to electricity. So, it could be very cost-efficient to use the existing power line infrastructure as part of the solution. These ideas have motivated us to analyze the performance of a dual-hop wireless-PLC mixed communication system employing decode-and-forward (DF) based relays in this paper.

The proposed system can assist wireless networks in reaching remote geographical areas through the ubiquitous power line infrastructure. This system model utilizes the benefits of both wireless and PLC technologies to provide last-mile and last-inch access to the consumers by reducing the cost overheads, particularly for smart grid and smart metering applications in rural and remote areas with low population densities. Such a system allows to extend the network coverage and provide internet access to any remote room in a building having an unused power socket but wireless signals cannot penetrate. This is particularly useful solution for TV set-top boxes, game consoles or computers, that need a continuous jitter-free wired connection but are located far from the router or in a different room altogether.

Another interesting realistic scenario is illustrated in Fig. 1 [34]. The wireless link serves as the access network part while the PLC link serves as the 'core network' part. Let us consider the process of accessing the internet using

the wireless network in a university. A router needs to be installed, then some dedicated wire needs to be laid out to connect the router with the outside internet. This means that once the wires have been laid out, it is difficult to change the location of the router. But with this wireless-PLC mixed approach, firstly, we do not have to lay out separate dedicated wires; secondly, we can add additional routers wherever needed, thereby adding to the flexibility of the communication system. For instance, in complex buildings (e.g., airports or high/big buildings), we may often find that the signal strength of Wi-Fi is quite weak, then it will be extremely convenient to increase the coverage of the access network using this approach. Hence, the considered system can effectively solve the range limitation issues of the conventional wireless communication systems.

PLC presents a huge scope in industrial scenarios as an alternative means for data transmission [35]. In industrial establishments, installing new communication systems for machines, controllers or sensors in old facilities or even communication with devices in farther locations with an already installed power line network pose a serious concern. The much lower installation time and costs coupled with the fact of not having to stop the plant for preparing the infrastructure make PLC an attractive solution for industry. Wireless communication has not gained good acceptance on the factory floor due to its limitation in achieving timely and successful packet transmission [36]. Further, in [37], a wireless transmitter (due to its failures and frequent stopping of the plant) was replaced with a broadband PLC solution to reduce the downtime of the plant to zero.

The proposed wireless-power line mixed system has some potential industrial applications as well. One potential industrial application is related to power line inspection. Currently, people may need to use helicopter to inspect the power line or people have to climb up to the tower to do the inspection, which is both costly and dangerous. However, there is a trend that drones are used to do this task. In this case, the drone can potentially transfer the information through the wire to the data center, which is located far away. This allows the drone to inspect longer distance in a cost-efficient way. Another possible industrial application of the proposed system is in structural health monitoring systems where a wireless sensor network (WSN) within the structure monitors different physical parameters (such as strain, loading, suspension, etc.) or environmental parameters (temperature, pressure, etc.). The data from the WSN is locally collected at the host structure from where it is forwarded to a remote server via PLC. This could be an important industrial application as engineering structures like bridges, wind turbines, oil and gas installations, power plants etc. are usually connected to a power line. Thus, wireless-power line mixed system could be an important solution for structural health monitoring systems in remote areas. The considered system can also be used in industrial automation and control, where the temperature and pressure data of boilers and reactors can be acquired using wireless medium and appropriate control signals could be sent via PLC link where manual operation could be hazardous.

Lampe and Han Vinck [38] have observed that a diversity gain cannot be attained by employing multi-hop cooperative PLC only links. The effects of multi-hop relaying on power line channel transfer function have been investigated in [39] and it has been experimentally shown that the presence of relaying nodes can intensify the attenuation and frequency selectivity, thereby having a negative effect on channel transfer function. Thus, these ideas have inspired us to study the wireless-power line mixed system model.

Contributions: Most of the works in literature focus on the performance of either dual-hop wireless systems [40], [41] or dual-hop PLC systems [42], [43]. In such systems, the performance analysis utilizes the simplicity arising due to the symmetry of system model as both the links are subjected to the same channel and noise. The performance of asymmetric dual-hop AF relaying systems in mixed Nakagami-m and Rician links is considered in [44], while the performance of hybrid satellite-terrestrial cooperative systems and hybrid satellite-FSO cooperative systems is detailed in [45] and [46], respectively. On the contrary, the work presented in this paper deals with the performance analysis of a mixed wireless and power line dual-hop system that has not been considered in literature so far to the best of authors' understanding. The analysis of such a system is not straightforward because we consider that the wireless link is corrupted by Nakagami-m fading and AWGN while the PLC link is subjected to Log-normal channel gain and Bernoulli-Gaussian noise, in contrast to the symmetric dual-hop systems considered in literature. Further, the effects of the impulsive noise have been incorporated in the analysis of the considered system, which, in itself, is a challenging task. The probability density function (pdf) of the equivalent end-to-end signal-to-noise ratio (SNR) of the proposed system is derived. We evaluate an approximate closed-form analytical expression of the average BER for the proposed system assuming M-ary PSK (M-PSK) modulation scheme. We also evaluate the diversity of the considered system through the high SNR analysis. Exact closed-form expression of the outage probability and an approximate closed-form expression of the capacity of the wireless-power line mixed system are also derived to provide further insights into the considered system.

The work presented in this paper is significantly different from [24] because in [24], only the BER performance of the wireless-power line mixed cooperative communication system was evaluated using the Gamma approximation to Log-normal distribution to simplify the BER analysis. However, in this paper, we obtain novel expressions for the outage probability as well as the capacity of the considered system in addition to the BER performance without employing the Gamma approximation to Log-normal distribution.

The rest of the paper is organized as follows. The wireless-power line mixed system model is discussed in Section II. In Section III, the performance of the considered system is evaluated in terms of the analytical average BER, outage

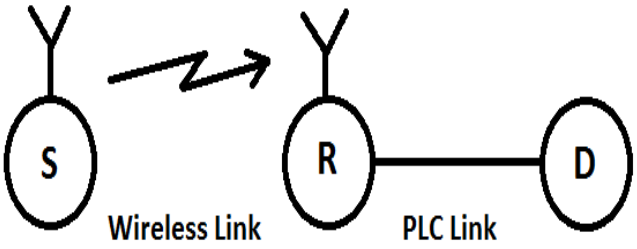

FIGURE 2. System model for a dual-hop wireless-power line mixed communication system with DF relay.

probability, and average channel capacity. Analytical and simulation results are discussed in Section IV and some conclusions are drawn in Section V.

II. SYSTEM DESCRIPTION

We consider a dual-hop cooperative communication system as shown in Fig. 2. M-PSK modulated data, s, are sent by the source (S) to the relay (R), which decodes and re-encodes the received data, and transmits this data to destination (D). R is equipped with a hybrid capability for interfacing wireless link with the PLC link. The wireless S-R link is characterized by Nakagami-m fading [20], [21] and AWGN. The PLC R-D link is subjected to Log-normally distributed channel gain [17], [18] and Bernoulli-Gaussian noise [10], [11]. The received signal at R is written as

$$r_w = h_w s + n_w, \tag{1}$$

where h_w incorporates the Nakagami-m fading of the wireless link having severity factor $m_w \in [0.5, \infty)$ and n_w represents AWGN having zero mean and σ_w^2 variance. The instantaneous SNR over the wireless link is $\gamma_w = |h_w|^2 E_s/\sigma_w^2 = (|h_w|^2 E_b \log_2 M_w)/\sigma_w^2 = |h_w|^2 \overline{\gamma_w}$, where E_s is the symbol energy, E_b is the bit energy, M_w is the constellation size, and $\overline{\gamma_w} = E_s/\sigma_w^2$. The pdf of γ_w is represented as

$$f_{\gamma_w}(\gamma) = \Big(\frac{m_w}{\overline{\gamma_w}}\Big)^{m_w} \frac{\gamma^{m_w-1}}{\Gamma(m_w)} \exp\Big(-\frac{m_w\gamma}{\overline{\gamma_w}}\Big). \tag{2}$$

The following input-output relation describes the received signal at D over the PLC link:

$$r_p = h_p \hat{s} + n_p, \tag{3}$$

where $\hat{s}$ is the signal decoded by R following DF relaying protocol. In (3), h_p is the PLC channel gain whose amplitude is distributed as

$$f(a_{h_p}) = \frac{1}{a_{h_p}\sqrt{2\pi\sigma_{h_p}^2}} e^{\left(-\frac{(\ln a_{h_p} - \mu_{h_p})^2}{2\sigma_{h_p}^2}\right)}, \tag{4}$$

where $a_{h_p} > 0$, μ_{h_p} and $\sigma_{h_p}^2$ are the mean and variance of the corresponding Gaussian random variable (RV) $\ln a_{h_p}$.[1]

[1]In this paper, we consider the specific case of a flat fading channel, in which the coherence time is larger than the frame length. As a result, the effect of channel state information (CSI) outdating, which happens due to Doppler spread that is related to the coherence time, does not play a role in this scenario.

The pdf of the additive noise on the PLC link is written as follows [10], [11]:

$$f(n_p) = (1-p)\mathcal{CN}(0, \sigma_g^2) + p\mathcal{CN}(0, \sigma_g^2 + \sigma_i^2). \tag{5}$$

Here $\mathcal{CN}(0, \sigma^2)$ stands for the complex Gaussian distribution having mean zero and σ^2 as variance and p is the arrival probability of the impulsive component of the Bernoulli-Gaussian noise. The noise power on the PLC link is σ_g^2 in the presence of only background noise; while the noise power is $\sigma_i^2 = \sigma_g^2(1+K)$ in the presence of both background and impulsive noises, where $K = \sigma_i^2/\sigma_g^2$ is the impulsive noise index. If γ_{p1} and γ_{p2} represent the instantaneous SNRs based on whether impulsive noise is absent or present on the PLC link, respectively, then the instantaneous SNR of the PLC link is expressed as

$$\begin{aligned}\gamma_p &= \begin{cases} \gamma_{p1} = \dfrac{|h_p|^2 E_{\hat{s}}}{\sigma_g^2}, & \text{only background noise,} \\ \gamma_{p2} = \dfrac{|h_p|^2 E_{\hat{s}}}{\sigma_g^2(1+K)}, & \text{with impulsive noise,} \end{cases} \\ &= \begin{cases} \gamma_{p1} = |h_p|^2 \overline{\gamma_p}, & \text{only background noise,} \\ \gamma_{p2} = |h_p|^2 \overline{\gamma_p}', & \text{with impulsive noise,} \end{cases} \end{aligned} \tag{6}$$

where $E_{\hat{s}}$ denotes the decoded symbol energy at R, $\overline{\gamma_p} = E_{\hat{s}}/\sigma_g^2 = (E_{\hat{b}} \log_2 M_p)/\sigma_g^2$, $E_{\hat{b}}$ is the decoded bit energy at R, M_p is the constellation size on the PLC link, and $\overline{\gamma_p}' = \overline{\gamma_p}/(K+1)$. The pdf of γ_p is written as

$$f_{\gamma_p}(\gamma) = \begin{cases} f_{\gamma_{p1}}(\gamma) & \text{only background noise,} \\ f_{\gamma_{p2}}(\gamma) & \text{with impulsive noise.} \end{cases} \tag{7}$$

It should be noted that $\gamma_{p1}(\gamma)$ and $\gamma_{p2}(\gamma)$ in (6), are also Log-normal RVs and their pdfs are given by

$$f_{\gamma_{p1}}(\gamma) = \frac{1}{\gamma\sqrt{2\pi\sigma'^2}} \exp\Big(-\frac{(\ln\gamma - \mu')^2}{2\sigma'^2}\Big), \tag{8}$$

$$f_{\gamma_{p2}}(\gamma) = \frac{1}{\gamma\sqrt{2\pi\sigma'^2}} \exp\Big(-\frac{(\ln\gamma - \mu'')^2}{2\sigma'^2}\Big), \tag{9}$$

where $\mu' = \ln\overline{\gamma_p} + 2\mu_{h_p}$, $\mu'' = \ln\overline{\gamma_p}' + 2\mu_{h_p}$, and $\sigma'^2 = 4\sigma_{h_p}^2$.

Remark 1: In this work, we have used fixed DF relaying protocol. A relay operating on incremental DF protocol could be used for congestion control. In this situation, the relay will be used only when the SNR of the source-destination link is very low and it receives a feedback from the destination in the form of an automatic repeat request (ARQ). The relay results in a more reliable end-to-end link and, hence, a reduction in the number of users losing their reserved time slots. This leads to a further reduction in the average number of contending users, and therefore, a much lower access delay. Alternatively, the relay could utilize multi-level priority scheduling approach to prioritize the data based on packet sizes, delivery speeds, and Quality of Service (QoS) needs. On a serial wireless-PLC link as considered in this manuscript, the PLC link could use orthogonal frequency division multiple access technique and would be time-sharing the available slots based on the priority of the data packets.

However, a detailed analysis of these schemes is beyond the scope of this work.

III. PERFORMANCE ANALYSIS

The end-to-end SNR of a DF based dual-hop cooperative system is the minimum of the SNRs of the individual links [47]. As a result, the equivalent end-to-end SNR of the considered wireless-PLC mixed communication system is expressed as follows:

$$\begin{aligned}\gamma_d &= \min(\gamma_w, \gamma_p)\\ &= \begin{cases}\gamma_{d1} & \text{only background noise,}\\ \gamma_{d2} & \text{with impulsive noise,}\end{cases}\end{aligned} \tag{10}$$

where $\gamma_{d1} = \min(\gamma_w, \gamma_{p1})$ is the end-to-end SNR in the absence of impulsive noise and $\gamma_{d2} = \min(\gamma_w, \gamma_{p2})$ is the end-to-end SNR when both types of additive noises are present. Further, using [48, eq. (6.81)] the cumulative distribution function (cdf), $F_{\gamma_{d1}}(\gamma)$ and $F_{\gamma_{d2}}(\gamma)$, of the equivalent SNR of the considered system is given by

$$\begin{aligned}F_{\gamma_{d1}}(\gamma) &= 1 - Pr[\gamma_{d1} > \gamma] = 1 - Pr[\gamma_w > \gamma, \gamma_{p1} > \gamma]\\ &= F_{\gamma_w}(\gamma) + F_{\gamma_{p1}}(\gamma) - F_{\gamma_w}(\gamma)F_{\gamma_{p1}}(\gamma), \qquad (11)\\ F_{\gamma_{d2}}(\gamma) &= F_{\gamma_w}(\gamma) + F_{\gamma_{p2}}(\gamma) - F_{\gamma_w}(\gamma)F_{\gamma_{p2}}(\gamma), \qquad (12)\end{aligned}$$

where $Pr[\cdot]$ denotes the probability. $F_{\gamma_w}(\gamma)$, $F_{\gamma_{p1}}(\gamma)$, and $F_{\gamma_{p2}}(\gamma)$ are calculated by integrating (2), (8), and (9), respectively, in the following manner:

$$F_{\gamma_w}(\gamma) = \frac{1}{\Gamma(m_w)}\gamma(m_w, \frac{m_w\gamma}{\overline{\gamma_w}}), \tag{13}$$

$$F_{\gamma_{p1}}(\gamma) = Q\Big(\frac{\mu' - \ln\gamma}{\sigma'}\Big), \tag{14}$$

$$F_{\gamma_{p2}}(\gamma) = Q\Big(\frac{\mu'' - \ln\gamma}{\sigma'}\Big), \tag{15}$$

where $\gamma(s,x) \triangleq \int_0^x t^{s-1}e^{-t}dt$, denotes the lower incomplete gamma function and $Q(x) \triangleq \frac{1}{\sqrt{2\pi}}\int_x^\infty \exp\Big(-\frac{t^2}{2}\Big)dt$, denotes the well-known Gaussian Q-function. On putting (13) and (14) in (11), and (13) and (15) in (12), respectively, we arrive at the desired cdfs, $F_{\gamma_{d1}}(\gamma)$ and $F_{\gamma_{d2}}(\gamma)$, of the equivalent SNR in the absence and presence of impulsive noise, respectively. The pdf of the equivalent SNRs for the considered scenarios is obtained by differentiating (11) and (12) with respect to γ, as follows:

$$\begin{aligned}f_{\gamma_{d1}}(\gamma) &= f_{\gamma_w}(\gamma) + f_{\gamma_{p1}}(\gamma) - f_{\gamma_w}(\gamma)F_{\gamma_{p1}}(\gamma)\\ &\quad - f_{\gamma_{p1}}(\gamma)F_{\gamma_w}(\gamma), \qquad (16)\\ f_{\gamma_{d2}}(\gamma) &= f_{\gamma_w}(\gamma) + f_{\gamma_{p2}}(\gamma) - f_{\gamma_w}(\gamma)F_{\gamma_{p2}}(\gamma)\\ &\quad - f_{\gamma_{p2}}(\gamma)F_{\gamma_w}(\gamma). \qquad (17)\end{aligned}$$

where $f_{\gamma_w}(\gamma)$, $f_{\gamma_{p1}}(\gamma)$, $f_{\gamma_{p2}}(\gamma)$, $F_{\gamma_w}(\gamma)$, $F_{\gamma_{p1}}(\gamma)$, and $F_{\gamma_{p2}}(\gamma)$ are given by (2), (8), (9), (13)-(15), respectively.

A. COMPUTATION OF BER

In this subsection, we evaluate the BER of M-PSK signals transmitted over the wireless-power line mixed cooperative system. By using the signal space concept, the BER as a function of instantaneous SNR is given by [49]

$$P_e\{\gamma\} \approx \frac{2}{\zeta_M}\sum_{k=1}^{\max(M/4,1)} Q(\sqrt{2\gamma}b_k), \tag{18}$$

where $\zeta_M = \max(\log_2 M, 2)$ and $b_k = \sin\Big(\frac{(2k-1)\pi}{M}\Big)$. Thus, the analytical average BER of the proposed system is expressed as

$$\begin{aligned}P_e &= (1-p)E_{\gamma_w,|h_p|^2}[P_e\{\min(\gamma_w, |h_p|^2\overline{\gamma_p})\}]\\ &\quad + pE_{\gamma_w,|h_p|^2}[P_e\{\min(\gamma_w, |h_p|^2\overline{\gamma_p}')\}], \qquad (19)\end{aligned}$$

where $E[\cdot]$ represents expectation. The average error probability in the presence of only background noise is obtained by using the order statistics as follows:

$$\begin{aligned}&E_{\gamma_w,|h_p|^2}[P_e\{\min(\gamma_w, |h_p|^2\overline{\gamma_p})\}]\\ &= \frac{2}{\zeta_{M_p}}\sum_{k=1}^{\max(M_p/4,1)}\int_0^\infty Q(\sqrt{2\gamma}b_{k_p})(1-F_{\gamma_w}(\gamma))f_{\gamma_{p_1}}(\gamma)d\gamma\\ &\quad + \frac{2}{\zeta_{M_w}}\sum_{k=1}^{\max(M_w/4,1)}\int_0^\infty Q(\sqrt{2\gamma}b_{k_w})(1-F_{\gamma_{p_1}}(\gamma))f_{\gamma_w}(\gamma)d\gamma,\end{aligned} \tag{20}$$

where $\zeta_{M_p} = \max(\log_2 M_p, 2)$, $b_{k_p} = \sin\Big(\frac{(2k-1)\pi}{M_p}\Big)$, $\zeta_{M_w} = \max(\log_2 M_w, 2)$, and $b_{k_w} = \sin\Big(\frac{(2k-1)\pi}{M_w}\Big)$. Similarly, when the impulsive noise is also present on the PLC link, the average error probability can be expressed as

$$\begin{aligned}&E_{\gamma_w,|h_p|^2}[P_e\{\min(\gamma_w, |h_p|^2\overline{\gamma_p}')\}]\\ &= \frac{2}{\zeta_{M_p}}\sum_{k=1}^{\max(M_p/4,1)}\int_0^\infty Q(\sqrt{2\gamma}b_{k_p})(1-F_{\gamma_w}(\gamma))f_{\gamma_{p_2}}(\gamma)d\gamma\\ &\quad + \frac{2}{\zeta_{M_w}}\sum_{k=1}^{\max(M_w/4,1)}\int_0^\infty Q(\sqrt{2\gamma}b_{k_w})(1-F_{\gamma_{p_2}}(\gamma))f_{\gamma_w}(\gamma)d\gamma.\end{aligned} \tag{21}$$

Using (20) and (21) in (19) and after some simplifications, P_e is given by

$$\begin{aligned}P_e &= (1-p)[P_{e1} + P_{e2} - P_{e3} - P_{e4}]\\ &\quad + p[P_{e1} + P_{e5} - P_{e6} - P_{e7}], \qquad (22)\end{aligned}$$

where $P_{e1} \approx \frac{2}{\zeta_{M_w}}\sum_{k=1}^{\max(M_w/4,1)}\int_0^\infty Q(\sqrt{2\gamma}b_{k_w})f_{\gamma_w}(\gamma)d\gamma$, $P_{e2} \approx \frac{2}{\zeta_{M_p}}\sum_{k=1}^{\max(M_p/4,1)}\int_0^\infty Q(\sqrt{2\gamma}b_{k_p})f_{\gamma_{p1}}(\gamma)d\gamma$, $P_{e3} \approx \frac{2}{\zeta_{M_w}}\sum_{k=1}^{\max(M_w/4,1)}\int_0^\infty Q(\sqrt{2\gamma}b_{k_w})f_{\gamma_w}(\gamma)F_{\gamma_{p1}}(\gamma)d\gamma$, $P_{e4} \approx \frac{2}{\zeta_{M_p}}\sum_{k=1}^{\max(M_p/4,1)}\int_0^\infty Q(\sqrt{2\gamma}b_{k_p})f_{\gamma_{p1}}(\gamma)F_{\gamma_w}(\gamma)d\gamma$, $P_{e5} \approx \frac{2}{\zeta_{M_p}}\sum_{k=1}^{\max(M_p/4,1)}\int_0^\infty Q(\sqrt{2\gamma}b_{k_p})f_{\gamma_{p2}}(\gamma)d\gamma$, $P_{e6} \approx \frac{2}{\zeta_{M_w}}\sum_{k=1}^{\max(M_w/4,1)}\int_0^\infty Q(\sqrt{2\gamma}b_{k_w})f_{\gamma_w}(\gamma)F_{\gamma_{p2}}(\gamma)d\gamma$, and $P_{e7} \approx \frac{2}{\zeta_{M_p}}\sum_{k=1}^{\max(M_p/4,1)}\int_0^\infty Q(\sqrt{2\gamma}b_{k_p})f_{\gamma_{p2}}(\gamma)F_{\gamma_w}(\gamma)d\gamma$. It should be noted that the cross-terms P_{e3}, P_{e4}, P_{e6}, and P_{e7}

become very small for all practical SNR values and can be ignored. Thus, P_e given by (22) can be approximated as

$$P_e \approx (1-p)[P_{e1}+P_{e2}]+p[P_{e1}+P_{e5}]. \tag{23}$$

Let us obtain the closed-form expression for each term in (23). On substituting the pdf of γ_w from (2) into P_{e1}, P_{e1} is written as

$$P_{e1} \approx \frac{2}{\zeta_{M_w}} \sum_{k=1}^{\max(M_w/4,1)} \int_0^{\infty} Q(\sqrt{2\gamma}b_{k_w}) \times \Big(\frac{m_w}{\overline{\gamma_w}}\Big)^{m_w} \frac{\gamma^{m_w-1}}{\Gamma(m_w)} \exp\Big(-\frac{m_w\gamma}{\overline{\gamma_w}}\Big)d\gamma. \tag{24}$$

Applying the transformation $\sqrt{\gamma}=t$ and using the definition $Q(x) \triangleq 1/2\,\mathrm{erfc}(x/\sqrt{2})$ in (24), we obtain

$$P_{e1} = \frac{2}{\zeta_{M_w}} \sum_{k=1}^{\max(M_w/4,1)} \frac{\Big(\frac{m_w}{\overline{\gamma_w}}\Big)^{m_w}}{\Gamma(m_w)} \int_0^{\infty} t^{2m_w-1} \times \exp\Big(-\frac{m_w t^2}{\overline{\gamma_w}}\Big)\mathrm{erfc}(b_{k_w}t)dt. \tag{25}$$

P_{e1}, in (25), can be solved using [50, eq. (2.8.5.6)], with $\alpha=2m_w$, $p=m_w/\overline{\gamma_w}$, and $c=b_{k_w}$, as follows:

$$P_{e1} = \frac{2}{\zeta_{M_w}} \sum_{k=1}^{\max(M_w/4,1)} \frac{\Big(\frac{m_w}{\overline{\gamma_w}}\Big)^{m_w}}{\Gamma(m_w)} \Big[\frac{\Gamma(m_w)}{2\Big(\frac{m_w}{\overline{\gamma_w}}\Big)^{m_w}} - \frac{b_{k_w}\Gamma(m_w+0.5)}{\sqrt{\pi}\Big(\frac{m_w}{\overline{\gamma_w}}\Big)^{m_w+0.5}} {}_2F_1\Big(\frac{1}{2}, m_w+\frac{1}{2}; \frac{3}{2}; \frac{-b_{k_w}^2\overline{\gamma_w}}{m_w}\Big)\Big]. \tag{26}$$

In (26), ${}_2F_1(\cdot,\cdot;\cdot;x)$ denotes Gaussian hypergeometric function [51, eq. (9.14.1)]. Now, P_{e2} is obtained by substituting $f_{\gamma_{p1}}(\gamma)$ in the expression for P_{e2} as follows:

$$\begin{aligned} P_{e2} &= \frac{2}{\zeta_{M_p}} \sum_{k=1}^{\max(M_p/4,1)} \int_0^{\infty} Q(\sqrt{2\gamma}b_{k_p}) \times \frac{1}{\gamma\sqrt{2\pi\sigma'^2}} \exp\Big(-\frac{(\ln\gamma-\mu')^2}{2\sigma'^2}\Big)d\gamma \\ &\approx \frac{2}{\zeta_{M_p}} \sum_{k=1}^{\max(M_p/4,1)} \frac{\eta_0}{\sqrt{2\pi\sigma'^2}} \exp\Big(\frac{-W_0\big(b_{k_p}^2 e^{\mu'}\sigma'^2\big)}{\sigma'^2} \times \Big[\eta_1\Big\{\frac{W_0\big(b_{k_p}^2 e^{\mu'}\sigma'^2\big)}{\sigma'^2}\Big\}^{\eta_2-1} + \frac{W_0\big(b_{k_p}^2 e^{\mu'}\sigma'^2\big)}{2}\Big]\Big), \end{aligned} \tag{27}$$

where (27) is obtained using [52, eq. (31)] and $W_0(\cdot)$ is the Lambert-W function. The parameters η_0, η_1, and η_2 are given by [52], [53]:

$$\begin{aligned} \eta_0 &= (0.06516(\sigma'+24.47))^2 - 2.5959, \\ \eta_1 &= -(0.06708(\sigma'-18.7231))^2 + 2.7904, \\ \eta_2 &= (0.03162(\sigma'-17.001))^2 + 0.662, \end{aligned}$$

for $\sigma'(dB) \in [2,6)$, whereas, for $\sigma'(dB) \in [6,12]$, the values are:

$$\begin{aligned} \eta_0 &= 0.258(\sigma'-6)+1.345, \\ \eta_1 &= -(0.0592(\sigma'-21.5))^2 + 2.9046, \\ \eta_2 &= (0.02646(\sigma'-20.07))^2 + 0.6434. \end{aligned}$$

The parameter, σ_{h_p} of the PLC channel depends on the communication environment and varies with the number of branching nodes in the PLC network and the center frequency [17], [19]. For the typical values of σ_{h_p} considered in [17] and [19] for a PLC channel, the value of $\sigma'(dB)$ falls in the above ranges. Hence, the approximation used in (27) is valid.

Moreover, P_{e5} is calculated by replacing μ' in the expression for P_{e2} with μ''. Substituting the expressions for P_{e1}, P_{e2}, and P_{e5} into (23), we obtain the required average BER of the system under consideration.

Remark 2: The analysis presented here can be extended to incorporate multicarrier format on the PLC link in future works using the concept outlined in [54] because sum of Log-normally distributed channel gains is another Log-normal RV [55]. This analysis is quite involved and beyond the scope of this work.

Let us perform the high SNR analysis for the BER in the following subsection.

B. ASYMPTOTIC BER ANALYSIS

For asymptotic BER analysis, we assume that $\overline{\gamma_w}=\overline{\gamma_p}$. Let us re-write P_{e1} given by (26) after some manipulations using [51, eq. (9.132.2)] as follows:

$$P_{e1} = \frac{2}{\zeta_{M_w}} \sum_{k=1}^{\max(M_w/4,1)} \Big[\frac{1}{2} - \frac{\Gamma(m_w+0.5)}{\sqrt{\pi}\Gamma(m_w)} \times \Big\{\frac{\Gamma(1.5)\Gamma(m_w)}{b_{k_w}\Gamma(m_w+0.5)} + \frac{\Gamma(1.5)\Gamma(-m_w)\Big(\frac{m_w}{\overline{\gamma}}\Big)^{m_w}}{\Gamma(0.5)\Gamma(1-m_w)b_{k_w}^{2m_w}} \times {}_2F_1\Big(m_w+0.5, m_w; m_w+1; \frac{-m_w}{b_{k_w}^2\overline{\gamma}}\Big)\Big\}. \tag{28}$$

Now, for high SNR, $\frac{-m_w}{b_{k_w}^2\overline{\gamma}} \to 0$, hence, ${}_2F_1(\cdot,\cdot;\cdot;x) \to 1$. Thus, P_{e1} can be approximated at high SNR as

$$P_{e1} \approx \frac{2}{\zeta_{M_w}} \sum_{k=1}^{\max(M_w/4,1)} \Big[\frac{1}{2} - \frac{\Gamma(m_w+0.5)}{\sqrt{\pi}\Gamma(m_w)} \times \Big\{\frac{\Gamma(1.5)\Gamma(m_w)}{b_{k_w}\Gamma(m_w+0.5)} + \frac{\Gamma(1.5)\Gamma(-m_w)\Big(\frac{m_w}{\overline{\gamma}}\Big)^{m_w}}{\Gamma(0.5)\Gamma(1-m_w)b_{k_w}^{2m_w}}\Big\}. \tag{29}$$

From (29), it is clear that P_{e1} falls with a slope of m_w at high SNR. The contribution of the PLC link in the expression for P_e occurs due to the terms P_{e2} and P_{e5}. Since the PLC link is subjected to Log-normal channel gain, it is established in literature [56] that for asymptotically large SNR, the diversity

order for Log-normal channels is ∞. Thus, the diversity order of the considered dual hop wireless-PLC system is $\min(m_w, \infty) = m_w$. This result is also verified through the plots shown in Fig. 7.

C. COMPUTATION OF OUTAGE PROBABILITY

The outage probability is that value of probability where the equivalent SNR falls below a particular threshold SNR, γ_{th}. Therefore, using (11) and (12), the outage probability of the considered system based on DF relaying protocol is written as

$$\begin{aligned} P_{out} &= F_{\gamma_d}(\gamma_{th}) \\ &= (1-p)F_{\gamma_{d1}}(\gamma_{th}) + pF_{\gamma_{d2}}(\gamma_{th}) \\ &= (1-p)\{F_{\gamma_w}(\gamma_{th}) + F_{\gamma_{p1}}(\gamma_{th}) - F_{\gamma_w}(\gamma_{th})F_{\gamma_{p1}}(\gamma_{th})\} \\ &\quad + p\{F_{\gamma_w}(\gamma_{th}) + F_{\gamma_{p1}}(\gamma_{th}) - F_{\gamma_w}(\gamma_{th})F_{\gamma_{p2}}(\gamma_{th})\}, \end{aligned} \tag{30}$$

where $F_{\gamma_w}(\gamma_{th})$, $F_{\gamma_{p1}}(\gamma_{th})$, and $F_{\gamma_{p2}}(\gamma_{th})$ are obtained by replacing γ with γ_{th} in (13)-(15).

D. COMPUTATION OF AVERAGE CHANNEL CAPACITY

In this subsection, we derive a closed-form expression of the average channel capacity of the considered dual-hop DF based wireless-power line mixed cooperative system. The average channel capacity, C is given by [57, eq. (13)]

$$\begin{aligned} C &= \frac{1}{2}\int_0^\infty \log_2(1+\gamma) f_{\gamma_d}(\gamma) d\gamma \\ &= \frac{(1-p)}{2\ln 2}\int_0^\infty \ln(1+\gamma) f_{\gamma_{d1}}(\gamma) d\gamma \\ &\quad + \frac{p}{2\ln 2}\int_0^\infty \ln(1+\gamma) f_{\gamma_{d2}}(\gamma) d\gamma. \end{aligned} \tag{31}$$

Now, using (16) and (17) in (31) and after some manipulations, C can be evaluated as

$$\begin{aligned} C &= \frac{(1-p)}{2\ln 2}(C_1 + C_2 - C_3 - C_4) \\ &\quad + \frac{p}{2\ln 2}(C_1 + C_5 - C_6 - C_7). \end{aligned} \tag{32}$$

We will now compute closed-form expressions for C_i, $i = \{1, 2, 3, 4, 5, 6, 7\}$. C_1 can be evaluated as

$$\begin{aligned} C_1 &= \int_0^\infty \ln(1+\gamma) f_{\gamma_w}(\gamma) d\gamma \\ &= \int_0^\infty \ln(1+\gamma) \Big(\frac{m_w}{\overline{\gamma_w}}\Big)^{m_w} \frac{\gamma^{m_w-1}}{\Gamma(m_w)} \exp\Big(-\frac{m_w\gamma}{\overline{\gamma_w}}\Big) d\gamma. \end{aligned} \tag{33}$$

The $\ln(\cdot)$ and $\exp(\cdot)$ functions in (33) can be expressed in terms of the Meijer-G function using [58, eq. (8.4.6.4)] and [58, eq. (8.4.3.1)], respectively, as

$$\begin{aligned} C_1 = \Big(\frac{m_w}{\overline{\gamma_w}}\Big)^{m_w} \frac{1}{\Gamma(m_w)} \int_0^\infty \gamma^{m_w-1} G_{0,1}^{1,0}\left(\frac{m_w\gamma}{\overline{\gamma_w}} \,\middle|\, \begin{matrix} - \\ 0 \end{matrix}\right) \\ \times G_{2,2}^{1,2}\left(\gamma \,\middle|\, \begin{matrix} 1, 1 \\ 1, 0 \end{matrix}\right) d\gamma. \end{aligned} \tag{34}$$

In (34), $G(\cdot|\ :)$ denotes the Meijer-G function [58, eq. (8.2.1)]. The integration in (34) can be solved using [59, eq. (07.34.21.0011.01)] in the following way

$$C_1 = \frac{1}{\Gamma(m_w)} G_{3,2}^{1,3}\left(\frac{\overline{\gamma_w}}{m_w} \,\middle|\, \begin{matrix} 1, 1, 1-m_w \\ 1, 0 \end{matrix}\right). \tag{35}$$

C_2 can be derived as follows:

$$\begin{aligned} C_2 &= \int_0^\infty \ln(1+\gamma) f_{\gamma_{p1}}(\gamma) d\gamma \\ &= \int_0^\infty \frac{\ln(1+\gamma)}{\gamma\sqrt{2\pi\sigma'^2}} \exp\Big(-\frac{(\ln\gamma - \mu')^2}{2\sigma'^2}\Big) d\gamma \\ &\approx \ln\Big[2\cosh\Big(\frac{\ln\overline{\gamma_p} + \mu'}{2}\Big)\Big] \\ &\quad + \frac{1}{2}\Bigg[\ln\overline{\gamma_p} + \mu' + \frac{\eta_0' \ln 10}{10\cosh^{\eta_1'}\Big(\frac{\ln\overline{\gamma_p} + \mu'}{2\eta_2'}\Big)}\Bigg], \end{aligned} \tag{36}$$

where (36) is obtained using [60, eq. (13)] after some simplifications. For $\sigma' \in [0.01, 6)$ dB, the parameters η_0' and η_1' are given by [60, eq. (13)]:

$$\begin{aligned} \eta_0' &= (-1.0658 \times 10^{-4}\sigma'^3 - 0.0019047\sigma'^2 \\ &\quad + 0.083954\sigma' - 0.0004047)\sigma'/\sqrt{2}, \\ \eta_1' &= -0.0160\sigma'^2 + 0.3180\sigma' + 1.6580, \end{aligned}$$

whereas, for $\sigma' \in [6, 12]$ dB, these parameters are written as

$$\begin{aligned} \eta_0' &= (8.7552 \times 10^{-5}\sigma'^3 - 0.0043629\sigma'^2 \\ &\quad + 0.093625\sigma' - 0.011684)\sigma'/\sqrt{2}, \\ \eta_1' &= -0.0080\sigma'^2 + 0.2200\sigma' + 1.9580. \end{aligned}$$

For $\sigma' \in [0.01, 12]$ dB, $\eta_2' = (0.045\sigma' + 0.385)\ln(10)$. The expression for C_5 is similar to the expression for C_2 but $\overline{\gamma_p}$ and μ' in (36) are replaced with $\overline{\gamma_p}'$ and μ'', respectively, for C_5. Now C_3 can be evaluated as

$$\begin{aligned} C_3 &= \int_0^\infty \ln(1+\gamma) f_{\gamma_w}(\gamma) F_{\gamma_{p1}}(\gamma) d\gamma \\ &= \int_0^\infty \ln(1+\gamma) \Big(\frac{m_w}{\overline{\gamma_w}}\Big)^{m_w} \frac{\gamma^{m_w-1}}{\Gamma(m_w)} \exp\Big(-\frac{m_w\gamma}{\overline{\gamma_w}}\Big) \\ &\quad \times Q\Big(\frac{\mu' - \ln\gamma}{\sigma'}\Big) d\gamma. \end{aligned} \tag{37}$$

On substituting $\big(\frac{m_w\gamma}{\overline{\gamma_w}}\big) = t$ in (37), C_3 becomes

$$C_3 = \int_0^\infty e^{-t} f(t) dt, \tag{38}$$

where

$$f(t) = \frac{t^{m_w-1}}{\Gamma(m_w)} \ln\Big(1 + \frac{\overline{\gamma_w} t}{m_w}\Big) Q\Big(\frac{\mu' - \ln\big(\frac{\overline{\gamma_w} t}{m_w}\big)}{\sigma'}\Big). \tag{39}$$

Utilising [61, eq. (25.4.45)], C_3 is expressed as

$$C_3 = \sum_{i=1}^{n} w_i f(t_i), \tag{40}$$

where t_i is the i^{th} zero of the Laguerre polynomial, $L_n(x)$, and the weights w_i's are calculated as follows:

$$w_i = \frac{(n!)^2 t_i}{(n+1)^2 [L_{n+1}(t_i)]^2}. \tag{41}$$

Let us now evaluate C_4, which is given by

$$\begin{aligned} C_4 &= \int_0^\infty \ln(1+\gamma) f_{\gamma_{p1}}(\gamma) F_{\gamma_w}(\gamma) d\gamma \\ &= \int_0^\infty \frac{\ln(1+\gamma)}{\gamma \sqrt{2\pi\sigma'^2}} \exp\Big(-\frac{(\ln\gamma - \mu')^2}{2\sigma'^2}\Big) \\ &\quad \times \frac{1}{\Gamma(m_w)} \gamma\Big(m_w, \frac{m_w \gamma}{\overline{\gamma_w}}\Big) d\gamma. \end{aligned} \tag{42}$$

Applying the transformation $\frac{\ln\gamma - \mu'}{\sqrt{2}\sigma'} = u$ and appropriately changing the limits of integration, C_4 is re-written as

$$C_4 = \int_{-\infty}^{\infty} e^{-u^2} g(u) du. \tag{43}$$

In (43), $g(u)$ is given by

$$g(u) = \frac{\ln(1 + e^{(\sqrt{2}\sigma' u + \mu')})}{\sqrt{\pi}\Gamma(m_w)} \gamma\Big(m_w, \frac{m_w}{\overline{\gamma_w}} e^{(\sqrt{2}\sigma' u + \mu')}\Big). \tag{44}$$

C_4 is derived with the aid of [61, eq. (25.4.46)] as

$$C_4 = \sum_{i=1}^{n} w_i' g(u_i), \tag{45}$$

where u_i is the i^{th} zero of the Hermite polynomial, $H_n(x)$, and the corresponding weight w_i' is calculated in the following way:

$$w_i' = \frac{2^{n-1} n! \sqrt{\pi}}{n^2 [H_{n-1}(u_i)]^2}. \tag{46}$$

C_6 and C_7 are solved on similar lines as described above by replacing μ' with μ'' in the expressions for C_3 and C_4, respectively.

Substituting the expressions for C_i, $i = \{1, 2, 3, 4, 5, 6, 7\}$ into (32), we get the analytical average capacity of the proposed communication system. The Meijer-G function used in (35) can be easily implemented using the in-built functions in Mathematica.

Discussion: The analytical results presented here pave the way for future research ideas. For instance, in the relay-enabled wireless-PLC system considered in [25, Fig. 1], each slave node will set its corresponding relay node accordingly with the best BER, after comparing the BERs of different relay nodes. All slave nodes belonging to the same relay node are called a cluster. Each node in the same cluster reports to its relay node by using CSMA/CA. The results derived above can be used in another useful scenario where a relay is equipped with both wireless as well PLC interfaces at its receiving and transmitting ends. The relay would estimate the link with the best SNR and would forward the data on that link. Our results could then be used to estimate the end-to-end performance. Further, the derived results can be utilized to design optimum resource allocation policies so that throughput of the system is maximized and at the same time meeting the QoS requirements based on power and BER constraints.

TABLE 1. Parameter values used for simulations.

Parameter	Values used
p	0.001, 0.05, 0.1, 0.15
K	10, 15, 20, 50, 100
$\sigma'(dB)$	1.5, 4
m_w	1, 1.5, 2, 3, 4
γ_{th}	5, 10
M_w	2
M_p	2, 4, 8
μ_{h_p}	0.5, 1

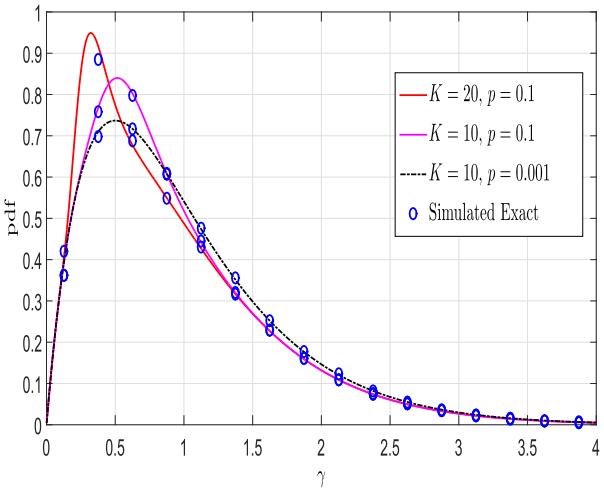

FIGURE 3. Comparison of analytical and simulated equivalent SNR pdf for various parameter values.

IV. NUMERICAL RESULTS AND DISCUSSIONS

The analytical results derived in the previous sections are discussed in this section. The results presented in the paper provide an insight into the performance of the system by showing the trends in the average BER, outage probability, and capacity with the variation of the system parameters such as m_w, K, p, etc. As a result, the behavior of the proposed system as predicted by these plots can be utilized in the design of a real system. We have provided the values for the different parameters used in the simulations in Table-1 for clarity. Some parameter values in Table-1 are available in literature [53], [62]–[64], while the others have been chosen so as to observe the trends and behavior of the proposed system for a better understanding. We have assumed that the average SNR per bit of the wireless link, E_b/σ_w^2, is equal to the average SNR per bit of the PLC link, $E_{\hat{b}}/\sigma_g^2$. We represent this average SNR along the x-axis from Fig. 3 onwards.

The pdf of the equivalent end-to-end SNR of the proposed system is shown for values of K and p for $m_w = 2$ and $\sigma'(dB) = 1.5$ in Fig. 3. The numerical plots are obtained using (16) and (17). We observe that the simulated pdf closely follows the derived pdf, for all considered values of

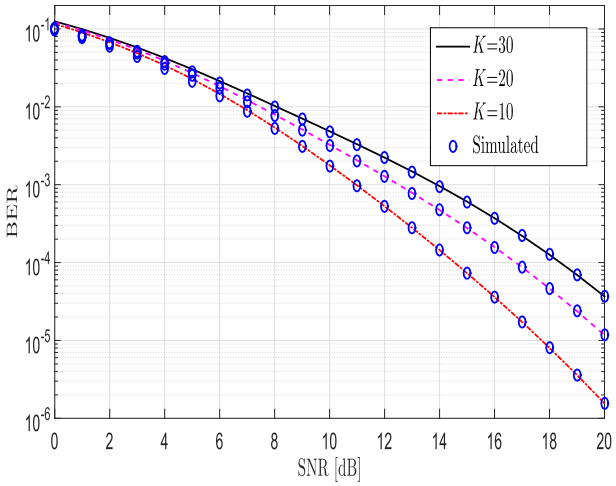

FIGURE 4. Comparison of analytical and simulated BER for various values of K with fixed $\sigma'(dB) = 4$, $m_W = 4$, and $p = 0.1$ assuming BPSK modulation.

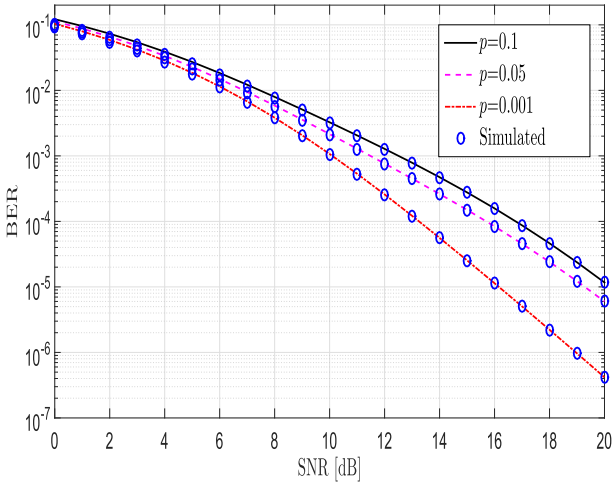

FIGURE 5. Comparison of analytical and simulated BER for various values of p with constant $K = 20$, $\sigma'(dB) = 4$, and $m_W = 4$ assuming BPSK modulation.

these parameters. It is clear from Fig. 3 that the peak value of the SNR pdf increases as K is varied from 10 to 20, i.e., the pdf becomes peaky as K becomes large. A similar trend is observed as the parameter p is increased from 0.001 to 0.1.

In Fig. 4, we compare the simulated and analytical BERs of the proposed wireless-power line mixed communication system for fixed $\sigma'(dB) = 4$, $m_w = 4$, and $p = 0.1$ by varying the parameter, K. The simulations are performed with the help of Monte Carlo method. The computational BER curves are plotted using (23). The validity of our derived results is established by close matching with the simulation results as evident from the figure. It is observed that as the value of K increases, that is, when the power of the impulsive component in the Bernoulli-Gaussian noise rises, the BER performance of this system becomes poor. It is because the parameter K indicates the severity of the impulsive component of the PLC additive noise. Due to the fact that the background noise power is less compared to the impulsive noise power for larger K values, the impulsive noise deteriorates the system performance more drastically.

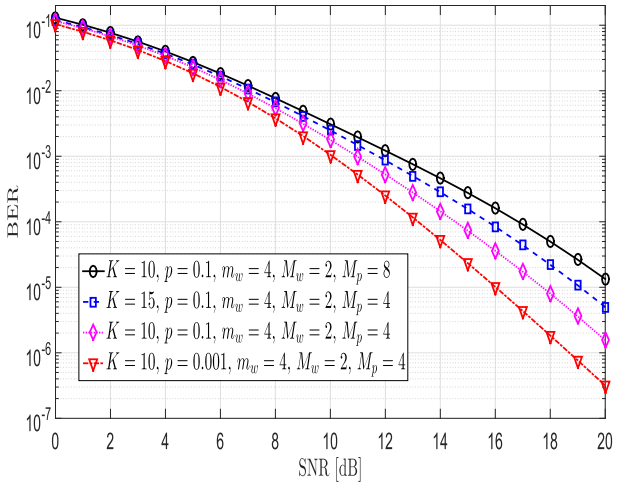

FIGURE 6. Comparison of analytical BER for various modulation schemes on the wireless and PLC links.

Fig. 5 explores the analytical BER of the proposed system for various values of probability of arrival of impulsive noise, p, for fixed values of $K = 20$, $\sigma'(dB) = 4$, and $m_w = 4$. Eq. (23) is used to obtain the computational BER plots. It is visible from Fig. 5 that with the increase in p from $p = 0.001$ to $p = 0.1$, the BER of the considered system gets worse. This is justified by noting that the impulsive component of the PLC additive noise is more harmful than the background noise. Thus, the impulsive noise more severely corrupts the transmitted data than the background noise. We observe from Fig. 5 that $p = 0.001$ corresponds to the weaker impulsive noise scenario on the PLC link. Hence, the BER is less when there is relatively weaker impulsive component in the Bernoulli-Gaussian noise compared to the heavy impulsive noise situation.

Fig. 6 shows a comparison of the analytical average BERs for different modulation schemes on the wireless and PLC links. The plots are obtained assuming BPSK modulation on the wireless link, i.e., $M_w = 2$. The figure indicates that the BER performance becomes poor as the value of M_p is increased from 4 to 8, while the other parameters are kept constant. The effect of the impulsive noise is again captured in Fig. 6 by observing the trends in the figure for various values of p and K. For instance, on increasing the impulsive noise index, K, from 10 to 15, the BER performance deteriorates as the transmitted data is corrupted by the impulsive noise. Similarly, the BER performance improves when p is less assuming a constant value for the other parameters.

A comparison of the analytical and asymptotic BER of the considered system for $K = 30$ and $p = 0.1$ for different values of m_w is shown in Fig. 7. It is seen that as the value of m_w increases the BER performance of the system improves because the severity of fading decreases with increasing m_w. We observe that the asymptotic BER curves match with the analytical BER curves. Further, it is noted from the figure that

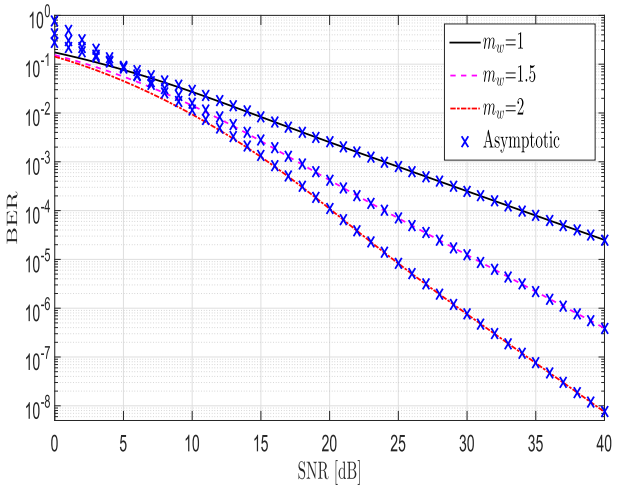

FIGURE 7. Comparison of analytical and asymptotic BER for various values of m_w assuming BPSK modulation.

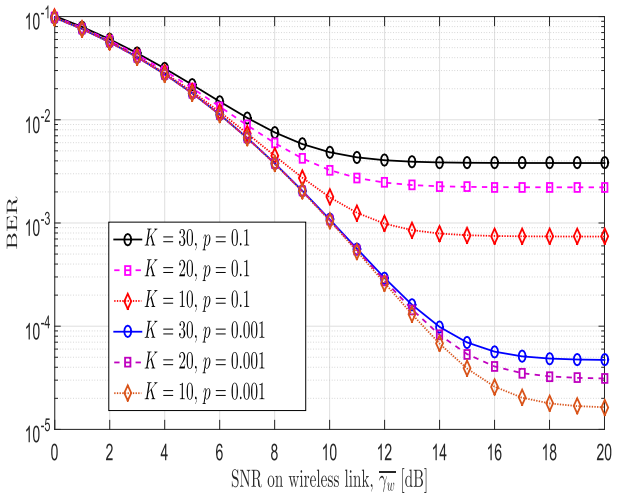

FIGURE 8. Effect of impulsive noise on the analytical BER for various values of p and K assuming BPSK modulation.

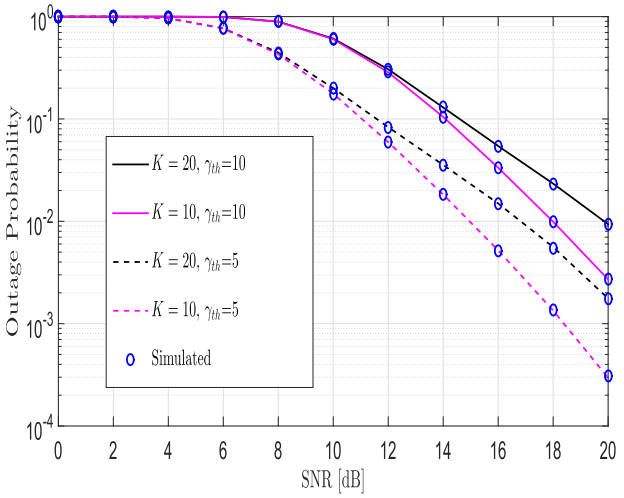

FIGURE 9. Comparison of analytical and simulated outage probability for various K and γ_{th} for fixed $p = 0.1$, $\sigma'(dB) = 4$, and $m_w = 4$.

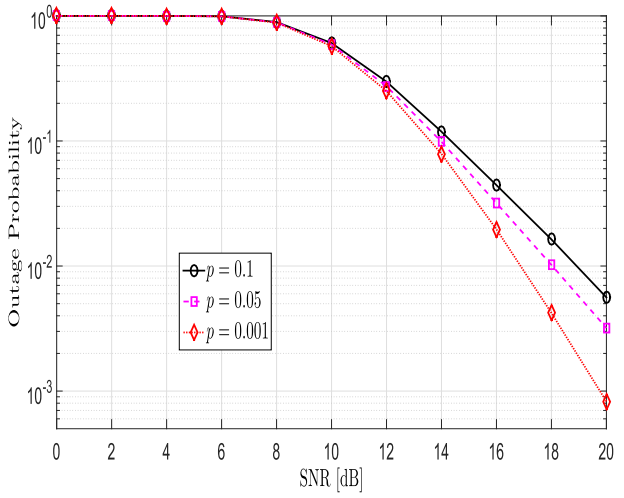

FIGURE 10. Comparison of outage probability for different values of p for fixed $K = 15$, $m_w = 3$, and $\gamma_{th} = 10$.

for $m_w = 1.5$ the BER is 1.233×10^{-5} at 30 dB SNR while it is 3.898×10^{-7} at 40 dB SNR. Thus, the BER falls with a slope of $\log_{10}(1.233 \times 10^{-5}) - \log_{10}(3.898 \times 10^{-7}) = 1.50012 \approx 1.5 = m_w$ at high SNR. Same conclusion can also be drawn from the curves corresponding to the other m_w values of 1 and 2. These results verify the analytical asymptotic analysis presented in Subsection III-B.

The effect of the severity of the impulsive noise is studied in more depth in Fig. 8 for different values of K and p assuming BPSK modulation on both the links. The signal to background noise power on the PLC link is fixed at 10 dB. It is evident from the figure that due to the deteriorating effect of the impulsive noise the BER does not improve with the increase in the average SNR on the wireless link. Thus, the impulsive noise results in loss in the diversity of the system. We also observe that the diversity loss occurs at a lower average SNR for higher value of the probability of arrival of impulsive noise.

In Fig. 9, we compare the analytical and simulated outage probability for the proposed system considering different K and γ_{th} values with fixed values of $p = 0.1$, $\sigma'(dB) = 4$, and $m_w = 4$. The simulation results have been obtained using Monte Carlo simulation while the computational curves have been plotted using (30). The simulation results closely match with analytical plots, thereby validating our analysis. It is evident from Fig. 9 that as the value of K decreases from $K = 20$ to $K = 10$, keeping the other parameters fixed, the outage probability decreases. It can also be observed from the figure that the outage probability degrades as the threshold value of the SNR, γ_{th}, increases from $\gamma_{th} = 5$ (or 6.9897 dB) to $\gamma_{th} = 10$ (or 10 dB). We infer from Fig. 9 that the outage probability curve for $K = 20$, $\gamma_{th} = 5$ will eventually cross over the outage probability curve for $K = 10$, $\gamma_{th} = 10$. This is quite intuitive because $K = 20$ implies that the impulsive noise index is quite high compared to $K = 10$. As a result, the outage performance for the case of $K = 20$, $\gamma_{th} = 5$ will eventually become poorer at high SNR. At low SNR, due to

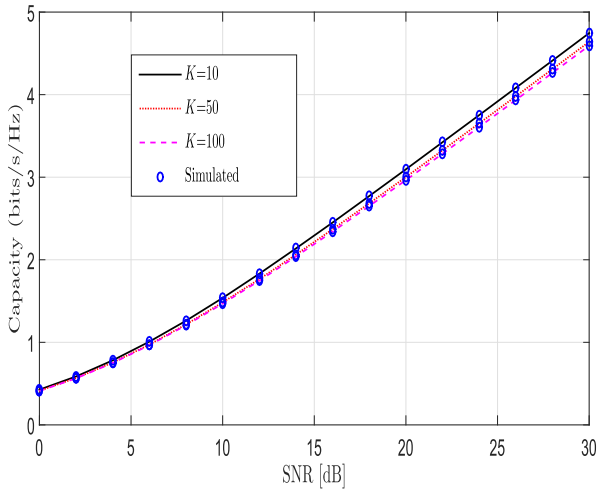

FIGURE 11. Average channel capacity versus SNR for various values of K for fixed $p = 0.1$, $\sigma'(dB) = 4$, and $m_w = 4$.

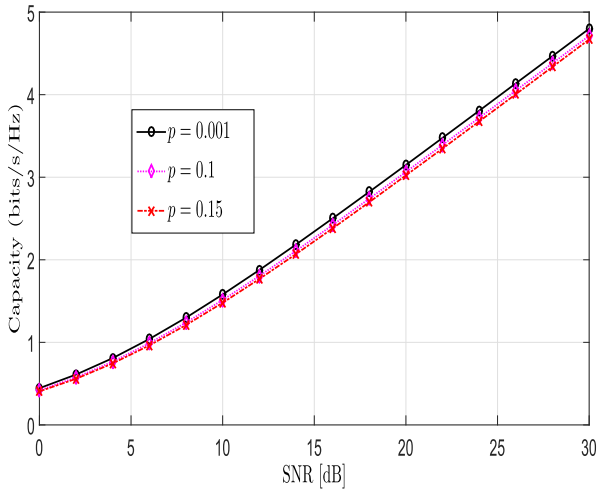

FIGURE 12. Average channel capacity versus SNR for various values of p with constant $K = 10$, $\sigma'(dB) = 4$, and $m_w = 3$.

lower value of $\gamma_{th} = 5$, the outage probability is lower for this case compared to $\gamma_{th} = 10$.

The outage probability of the considered system is plotted for different values of p for constant values of parameters $K = 15$, $\sigma'(dB) = 4$, $m_w = 3$, and $\gamma_{th} = 10$ in Fig. 10. We observe from the plot that as the arrival probability p of the impulsive component of PLC additive noise is raised from $p = 0.001$ to $p = 0.1$, the outage probability increases, that is, the system performance worsens.

In Fig. 11, the average channel capacity is plotted as a function of SNR for various values of the impulsive noise index K for $p = 0.1$, $\sigma'(dB) = 4$, and $m_w = 4$. The computational curves are obtained using the expression in (32). The adverse effect of impulsive noise is again visible in the capacity plot as we observe that the capacity of the system decreases as the power of the impulsive noise increases compared to the power of the background noise. An interesting observation can be made from Fig. 10. The capacity increases as we decrease the impulsive noise index from $K = 100$ to $K = 50$ but the increase is not much. This is because $K = 50$ and $K = 100$ are significantly high values of the impulsive noise index, which is capable of removing chunks of data on the PLC link. The performance of the considered system will be significantly deteriorated at such high values of K. Thus, even on reducing K from 100 to 50, the capacity does not improve that much.

In order to observe the variation of the average channel capacity with respect to the occurrence probability of the impulsive noise on the PLC link, we plot the average channel capacity as a function of SNR for different values of p for fixed $K = 10$, $\sigma'(dB) = 4$, and $m_w = 3$ in Fig. 12. As expected, the capacity of the system is better for lower values of p compared to higher values.

V. CONCLUSIONS

In this paper, we analyzed a novel dual-hop wireless-power line mixed communication system utilizing DF based relay. The pdf expression for the equivalent end-to-end SNR of the proposed system has been derived. We obtain an approximate closed-form expression of the analytical average BER for the system under consideration. Further, we obtain exact closed-form expression for the outage probability and an approximate expression of the average channel capacity of the system. It is inferred from the numerical plots that the arrival probability of the impulsive noise and the impulsive noise index parameter of the additive noise on the PLC link adversely impact the behavior of the proposed cooperative communication system. Useful insights into the system performance can be ascertained through the trends obtained in various numerical plots.

REFERENCES

[1] A. Majumder and J. Caffery, Jr., "Power line communications: An overview," *IEEE Potentials Mag.*, vol. 23, no. 4, pp. 4–8, Oct./Nov. 2004.
[2] H. Meng *et al.*, "Modeling of transfer characteristics for the broadband power line communication channel," *IEEE Trans. Power Del.*, vol. 19, no. 3, pp. 1057–1064, Jul. 2004.
[3] H. Meng, Y. L. Guan, and S. Chen, "Modeling and analysis of noise effects on broadband power-line communications," *IEEE Trans. Power Del.*, vol. 20, no. 2, pp. 630–637, Apr. 2005.
[4] Z. Tao, Y. Xiaoxian, Z. Baohui, N. H. Xu, F. Xiaoqun, and L. Changxin, "Statistical analysis and modeling of noise on 10-kV medium-voltage power lines," *IEEE Trans. Power Del.*, vol. 22, no. 3, pp. 1433–1439, Jul. 2007.
[5] H. Matsuo, D. Umehara, M. Kawai, and Y. Morihiro, "An iterative detection for OFDM over impulsive noise channel," in *Proc. 6th Int. Symp. Power-Line Commun. Appl. (ISPLC)*, 2002, pp. 203–207.
[6] V. B. Balakirsky and A. J. H. Vinck, "Potential limits on power—Line communication over impulsive noise channels," in *Proc. 7th Int. Symp. Power-Line Commun. Appl.*, 2003, pp. 32–36.
[7] A. Mathur and M. R. Bhatnagar, "PLC performance analysis assuming BPSK modulation over Nakagami-*m* additive noise," *IEEE Commun. Lett.*, vol. 18, no. 6, pp. 909–912, Jun. 2014.
[8] A. Mathur, M. R. Bhatnagar, and B. K. Panigrahi, "Maximum likelihood decoding of QPSK signal in power line communications over Nakagami-m additive noise," in *Proc. 19th IEEE Int. Symp. Power Line Commun. Appl. (ISPLC)*, Mar./Apr. 2015, pp. 7–12.
[9] A. Mathur, M. R. Bhatnagar, and B. K. Panigrahi, "Performance evaluation of PLC under the combined effect of background and impulsive noises," *IEEE Commun. Lett.*, vol. 19, no. 7, pp. 1117–1120, Jul. 2015.
[10] Y. H. Ma, P. L. So, and E. Gunawan, "Performance analysis of OFDM systems for broadband power line communications under impulsive noise and multipath effects," *IEEE Trans. Power Del.*, vol. 20, no. 2, pp. 674–682, Apr. 2005.

[11] L. D. Bert, P. Caldera, D. Schwingshackl, and A. M. Tonello, "On noise modeling for power line communications," in *Proc. IEEE Int. Symp. Power Line Commun. Appl. (ISPLC)*, Apr. 2011, pp. 283–288.

[12] J.-H. Lee, H.-S. Lee, J.-H. Park, and S.-C. Kim, "Measurement, modeling and simulation of power line channel for indoor high-speed data communications," in *Proc. 5th Int. Symp. Power-Line Commun. Appl.*, 2001, pp. 143–148.

[13] Y.-H. Kim, H.-H. Song, J.-H. Lee, and C.-S. Kim, "Wideband channel measurements and modeling for in-house power line communication," in *Proc. 6th Int. Symp. Power-Line Commun. Appl.*, 2002, pp. 1–5.

[14] M. Tlich, A. Zeddam, F. Moulin, and F. Gauthier, "Indoor power-line communications channel characterization up to 100 MHz—Part I: One-parameter deterministic model," *IEEE Trans. Power Del.*, vol. 23, no. 3, pp. 1392–1401, Jul. 2008.

[15] B. Tan and J. Thompson. *Powerline Communications Channel Modelling Methodology Based on Statistical Features*. Accessed: May 25, 2014. [Online]. Available: http://arxiv.org/pdf/1203.3879.pdf

[16] A. Mathur, M. R. Bhatnagar, and B. K. Panigrahi, "PLC performance analysis over Rayleigh fading channel under Nakagami-*m* additive noise," *IEEE Commun. Lett.*, vol. 18, no. 12, pp. 2101–2104, Dec. 2014.

[17] S. Guzelgoz, H. B. Celebi, and H. Arslan, "Statistical characterization of the paths in multipath PLC channels," *IEEE Trans. Power Del.*, vol. 26, no. 1, pp. 181–187, Jan. 2011.

[18] S. Galli, "A novel approach to the statistical modeling of wireline channels," *IEEE Trans. Commun.*, vol. 59, no. 5, pp. 1332–1345, May 2011.

[19] I. C. Papaleonidopoulos, C. N. Capsalis, C. G. Karagiannopoulos, and N. J. Theodorou, "Statistical analysis and simulation of indoor single-phase low voltage power-line communication channels on the basis of multipath propagation," *IEEE Trans. Consum. Electron.*, vol. 49, no. 1, pp. 89–99, Feb. 2003.

[20] H. Suzuki, "A statistical model for urban radio propogation," *IEEE Trans. Commun.*, vol. COMM-25, no. 7, pp. 673–680, Jul. 1977.

[21] A. U. Sheikh, M. Abdi, and M. Handforth, "Indoor mobile radio channel at 946 MHz: Measurements and modeling," in *Proc. 43rd IEEE Veh. Technol. Conf. (VTC)*, May 1993, pp. 73–76.

[22] E. Soleimani-Nasab, A. Kalantari, and M. Ardebilipour, "Performance analysis of multi-antenna df relay networks over Nakagami-*m* fading channels," *IEEE Commun. Lett.*, vol. 15, no. 12, pp. 1372–1374, Dec. 2011.

[23] E. Soleimani-Nasab, M. Matthaiou, and M. Ardebilipour, "Multi-relay MIMO systems with OSTBC over Nakagami-*m* fading channels," *IEEE Trans. Veh. Technol.*, vol. 62, no. 8, pp. 3721–3736, Oct. 2013.

[24] A. Mathur, M. R. Bhatnagar, and B. K. Panigrahi, "Performance of a dual-hop wireless-powerline mixed cooperative system," in *Proc. IEEE Int. Conf. Adv. Technol. Commun. (ATC)*, Oct. 2016, pp. 401–406.

[25] S. Lai and G. Messier, "The wireless/power-line diversity channel," in *Proc. IEEE Int. Conf. Commun. (ICC)*, May 2010, pp. 1–5.

[26] M. Kuhn, S. Berger, I. Hammerstrom, and A. Wittneben, "Power line enhanced cooperative wireless communications," *IEEE J. Sel. Areas Commun.*, vol. 24, no. 7, pp. 1401–1410, Jul. 2006.

[27] H. Bai, M. Li, D. Wang, L. Wang, and T. Zhao, "Relay-enabled hybrid wireless and powerline communication access network for smart power grid," in *Unifying Electrical Engineering and Electronics Engineering* (Lecture Notes in Electrical Engineering), vol. 238, S. Xing, S. Chen, Z. Wei, and J. Xia, Eds. New York, NY, USA: Springer, 2014.

[28] INSTEON Technology. (2013). *Whitepaper: The Details, v. 2.0*. Accessed: Oct. 16, 2017. [Online]. Available: http://www.insteon.net/pdf/insteondetails.pdf

[29] M. Rafiei and S. M. Eftekhari, "A practical smart metering using combination of power line communication (PLC) and WiFi protocols," in *Proc. 17th Conf. Electr. Power Distrib. Netw. (EPDC)*, May 2012, pp. 1–5.

[30] A. Mckeown, H. Rashvand, T. Wilcox, and P. Thomas, "Priority SDN controlled integrated wireless and powerline wired for smart-home Internet of Things," in *Proc. 12th IEEE Int. Conf. Autonomic Trusted Comput. 15th Int. Conf. Scalable Comput. Commun. Associated Workshops (UIC-ATC-ScalCom)*, Aug. 2015, pp. 1825–1830.

[31] T. R. Oliveira, A. G. Marques, M. S. Pereira, S. L. Netto, and M. V. Ribeiro, "The characterization of hybrid PLC-wireless channels: A preliminary analysis," in *Proc. 17th IEEE Int. Symp. Power-Line Commun. Appl. (ISPLC)*, Mar. 2013, pp. 98–102.

[32] F. Salvadori, C. S. Gehrke, A. C. de Oliveira, M. de Campos, and P. S. Sausen, "Smart grid infrastructure using a hybrid network architecture," *IEEE Trans. Smart Grid*, vol. 4, no. 3, pp. 1630–1639, Sep. 2013.

[33] *ICT Facts and Figures*. Accessed: Jan. 16, 2017. [Online]. Available: http://www.itu.int/en/ITU-D/Statistics/Documents/facts/ICTFactsFigures2015.pdf

[34] *Power Line Communication (PLC)*. Accessed: Jan. 16, 2017. [Online]. Available: https://seminarprojects.blogspot.com/2012/08/power-line-communication-plc.html

[35] S. C. Pereira, A. S. Caporali, and I. R. S. Casella, "Power line communication technology in industrial networks," in *Proc. 19th IEEE Int. Symp. Power Line Commun. Appl. (ISPLC)*, Mar./Apr. 2015, pp. 216–221.

[36] A. Willig, K. Matheus, and A. Wolisz, "Wireless technology in industrial networks," *Proc. IEEE*, vol. 93, no. 6, pp. 1130–1151, Jun. 2005.

[37] N. P. Queiroz, "Providing communication solutions in inhospitable industrial environments via PLC—A case study applied to a bauxite forklift at the Alunorte refinery," M.S. thesis, Dept. Elect. Eng., Federal Univ. Para, Belem, Brazil, 2009.

[38] L. Lampe and A. J. Han Vinck, "Cooperative multihop power line communications," in *Proc. 16th IEEE Int. Symp. Power Line Commun. Appl. (ISPLC)*, Mar. 2012, pp. 1–6.

[39] M. Rozman, A. Ikpehai, B. Adebisi, and K. M. Rabie, "Channel characterisation of cooperative relaying power line communication systems," in *Proc. 10th IEEE Int. Symp. Commun. Syst., Netw. Digit. Signal Process. (CSNDSP)*, Jul. 2016, pp. 1–5.

[40] O. S. Badarneh and R. Mesleh, "Cooperative dual-hop wireless communication systems with beamforming over η-μ fading channels," *IEEE Trans. Veh. Technol.*, vol. 65, no. 1, pp. 37–46, Jan. 2016.

[41] T. A. Tsiftsis, G. K. Karagiannidis, and S. A. Kotsopoulos, "Dual-hop wireless communications with combined gain relays," *IEE Proc.-Commun.*, vol. 153, no. 5, pp. 528–532, Oct. 2005.

[42] S. Ezzine, F. Abdelkefi, J. P. Cances, V. Meghdadi, and A. Bouallegue, "Capacity analysis of an OFDM-based two-hops relaying PLC systems," in *Proc. 81st IEEE Veh. Technol. Conf. (VTC Spring)*, May 2015, pp. 1–5.

[43] K. M. Rabie, B. Adebisi, and A. Salem, "Improving energy efficiency in dual-hop cooperative PLC relaying systems," in *Proc. 20th IEEE Int. Symp. Power Line Commun. Appl. (ISPLC)*, Mar. 2016, pp. 196–200.

[44] S. S. Soliman and N. C. Beaulieu, "Dual-hop AF relaying systems in mixed Nakagami-m and Rician links," in *Proc. IEEE Globecom Workshops*, Dec. 2012, pp. 447–452.

[45] M. K. Arti and M. R. Bhatnagar, "Beamforming and combining in hybrid satellite-terrestrial cooperative systems," *IEEE Commun. Lett.*, vol. 18, no. 3, pp. 483–486, Mar. 2014.

[46] M. R. Bhatnagar and M. K. Arti, "Performance analysis of hybrid satellite-terrestrial FSO cooperative system," *IEEE Photon. Technol. Lett.*, vol. 25, no. 22, pp. 2197–2200, Nov. 15, 2013.

[47] T. Wang, A. Cano, G. B. Giannakis, and J. N. Laneman, "High-performance cooperative demodulation with decode-and-forward relays," *IEEE Trans. Commun.*, vol. 55, no. 7, pp. 1427–1438, Jul. 2007.

[48] A. Papoulis and S. U. Pillai, *Probability, Random Variables and Stochastic Processes*, 4th ed. New York, NY, USA: McGraw-Hill, 2002.

[49] J. Lu, K. B. Letaief, J. C.-I. Chuang, and M. L. Liou, "M-PSK and M-QAM BER computation using signal-space concepts," *IEEE Trans. Commun.*, vol. 47, no. 2, pp. 181–184, Feb. 1999.

[50] Y. A. Brychkov, O. I. Marichev, and A. P. Prudnikov, *Integrals and Series*, vol. 2. New York, NY, USA: Gordon and Breach Science Publishers, 1992.

[51] I. S. Gradshteyn and I. M. Rhyzhik, *Table of Integrals, Series, and Products*, 7th ed., A. Jeffrey and D. Zwillinger, Eds. Burlington, MA, USA: Academic, 2007.

[52] F. Heliot, M. Ghavami, and M. R. Nakhai, "An accurate closed-form approximation of the average probability of error over a log-normal fading channel," *IEEE Trans. Wireless Commun.*, vol. 7, no. 5, pp. 1495–1500, May 2008.

[53] A. Dubey, R. K. Mallik, and R. Schober, "Performance of a PLC system in impulsive noise with selection combining," in *Proc. IEEE Glob. Commun. Conf. (GLOBECOM)*, Dec. 2012, pp. 3508–3512.

[54] Z. Du, J. Cheng, and N. C. Beaulieu, "Accurate error-rate performance analysis of OFDM on frequency-selective Nakagami-m fading channels," *IEEE Trans. Commun.*, vol. 54, no. 2, pp. 319–328, Feb. 2006.

[55] J. C. S. Filho, P. Cardieri, and M. D. Yacoub, "Simple accurate lognormal approximation to lognormal sums," *Electron. Lett.*, vol. 41, no. 18, pp. 1016–1017, Sep. 2005.

[56] X. Song, J. Cheng, and S.-M. Alouini, "High SNR BER comparison of coherent and differentially coherent modulation schemes in lognormal fading channels," *IEEE Commun. Lett.*, vol. 18, no. 9, pp. 1507–1510, Sep. 2014.

[57] S. Anees and M. R. Bhatnagar, "On the capacity of decode-and-forward dual-hop free space optical communication systems," in *Proc. IEEE Wireless Commun. Netw. Conf. (WCNC)*, Apr. 2014, pp. 18–23.
[58] Y. A. Brychkov, O. I. Marichev, and A. P. Prudnikov, *Integrals and Series*, vol. 3. New York, NY, USA: Gordon and Breach Science Publishers, 1990.
[59] Wolfram Research Inc., Champaign, IL, USA. *Meijer G*. Accessed: May 27, 2017. [Online]. Available: http://functions.wolfram.com/HypergeometricFunctions/MeijerG/
[60] F. Heliot, X. Chu, R. Hoshyar, and R. Tafazolli, "A tight closed-form approximation of the log-normal fading channel capacity," *IEEE Trans. Wireless Commun.*, vol. 8, no. 6, pp. 2842–2847, Jun. 2009.
[61] M. Abromowitz and I. A. Stegun, *Handbook of Mathematical Functions with Formulas, Graphs, and Mathematical Tables*. New York, NY, USA: Dover, 1970.
[62] N. C. Beaulieu and C. Cheng, "An efficient procedure for Nakagami-m fading simulation," in *Proc. IEEE Global Commun. Conf. (GLOBECOM)*, Nov. 2001, pp. 3336–3342.
[63] J. D. Parsons, *The Mobile Radio Propagation Channel*, 2nd ed. New York, USA: Wiley, 2000.
[64] A. Dubey, D. Sharma, R. K. Mallik, and S. Mishra, "Modeling and performance analysis of a PLC system in presence of impulsive noise," in *Proc. IEEE Power Energy Soc. Gen. Meeting*, Jul. 2015, pp. 1–5.

AASHISH MATHUR (S'14–M'17) received the B.E. degree (Hons.) in electronics and instrumentation engineering from the Birla Institute of Technology and Science, Pilani, Pilani, Rajasthan, India, in 2011, the M.Tech. degree in telecommunication technology and management from IIT Delhi, New Delhi, India, in 2013, and the Ph.D. degree in power line communications from the Department of Electrical Engineering, IIT Delhi. He was a Software Engineer with Intel Technology India Pvt. Ltd., Bangalore, India. He is currently an Assistant Professor with the Department of Electrical Engineering, IIT Jodhpur, India. His research interests include power line communications, visible light communications, and free-space optical communications.

MANAV R. BHATNAGAR (M'04–SM'13) received the M.Tech. degree in communication engineering from the IIT Delhi, New Delhi, India, in 2005, and the Ph.D. degree in wireless communications from the Department of Informatics, University of Oslo, Oslo, Norway, in 2008. From 2008 to 2009, he was a Post-Doctoral Research Fellow with the University Graduate Center (UNIK), University of Oslo. He held visiting appointments with the Wireless Research Group, IIT Delhi; the Signal Processing in Networking and Communications Group, University of Minnesota Twin Cities, Minneapolis, MN, USA; the Alcatel-Lucent Chair, SUPELEC, France; the Department of Electrical Computer Engineering, Indian Institute of Science, Bangalore, India; UNIK, University of Oslo; the Department of Communications and Networking, Aalto University, Espoo, Finland; and the INRIA/IRISA Laboratory, University of Rennes, Lannion, France. He is currently an Associate Professor with the Department of Electrical Engineering, IIT Delhi. His research interests include signal processing for multiple-input-multiple-output systems, cooperative communications, non-coherent communication systems, distributed signal processing for cooperative networks, multiuser communications, ultra-wideband-based communications, free-space optical communication, cognitive radio, software-defined radio, power line communications, and satellite communications. He is a Fellow of the Institution of Engineering and Technology, U.K., the Indian National Academy of Engineering, the Institution of Electronics and Telecommunication Engineers, India, and the Optical Society of India. He has received the NASI-Scopus Young Scientist Award 2016 in engineering category and the Shri Om Prakash Bhasin Award in the field of electronics and information technology for the year 2016. He was selected as an Exemplary Reviewer of the IEEE COMMUNICATIONS LETTERS for 2010 and 2012, and an Exemplary Reviewer of the IEEE TRANSACTIONS ON COMMUNICATIONS for 2015. He was an Editor of the IEEE TRANSACTIONS ON WIRELESS COMMUNICATIONS from 2011 to 2014.

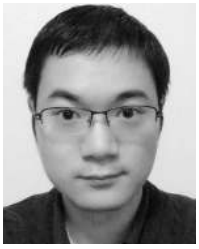

YUN AI (S'15–M'18) received the M.Sc. degree in electrical engineering from the Chalmers University of Technology, Göteborg, Sweden, in 2012, and the Ph.D. degree from the University of Oslo, Oslo, Norway, in 2018. In 2016, he was a Visiting Researcher with the Department of Information and Computer Science, Keio University, Tokyo, Japan. In 2016, funded by a stipend from the Norwegian University Center in St. Petersburg, Russia, he was a Visiting Researcher with the Faculty of Applied Mathematics and Control Processes, Saint Petersburg State University, Saint Petersburg, Russia. He is currently a Researcher with the Norwegian University of Science and Technology, Norway. He has also been with the Signal Processing Group, Technische Universität Darmstadt, Darmstadt, Germany, as a Research Student. His current research interests include the broad areas of wireless communications with focuses on radio propagation modeling, wireless sensor network, and smart grid.

MICHAEL CHEFFENA received the M.Sc. degree in electronics and computer technology from the University of Oslo, Oslo, Norway, in 2005, and the Ph.D. degree in telecommunications from the Norwegian University of Science and Technology (NTNU), Trondheim, Norway, in 2008. He was a Visiting Researcher with the Communications Research Center, Ottawa, ON, Canada, in 2007. From 2009 to 2010, he conducted his post-doctoral study at the University Graduate Center, Kjeller, Norway, and the French Space Agency, Toulouse, France. He is currently a Full Professor with NTNU. His current research interests include the modeling and prediction of radio channels for both terrestrial and satellite links, and medium access control protocol design.